

# A novel detection method of periodically moving region in radial MRI

Hyunseok Seo and HyunWook Park

Department of Electrical Engineering, KAIST / Daejeon 305-701 South Korea  
hsseo@athena.kaist.ac.kr, hwpark@kaist.ac.kr

\* Corresponding Author: HyunWook Park

Received May 13, 2013; Revised May 28, 2013; Accepted June 12, 2013; Published August 31, 2013

\* Short Paper

**Abstract:** The appropriate handling of motion artifacts is essential for clinical diagnosis in magnetic resonance imaging (MRI). In many cases, motion is an inherent part of MR images because it is difficult to control during MR imaging. As the motion in the human body occur in a deformable manner, they are difficult to deal with. This paper proposes a novel detection method for periodically moving regions to produce MR images with less motion artifacts. When the data is acquired by the radial trajectory, the proposed method can extract the deformable region easily using the difference in the modulated sinograms, which have different periodic phase terms. The simulation results applied to the various cases confirmed the good performance of the proposed method.

**Keywords:** Image processing, Motion correction, Projection reconstruction, Radial MRI, Respiratory, Sinogram

## 1. Introduction

Dealing with motion artifacts is a very important issue in medical imaging [1, 2] because patients are always in motion, such as tossing, turning, breathing, and cardiac pulsatile motions. These motions can appear as severe artifacts in the images. Motion can be largely classified into two categories: translational motion and deformable motion [3]. A vast amount of research results on translational motions that provide modeling tactics and technical solutions have been published [4] and the artifacts due to translational motion can be eliminated rather easily. In addition, most of translational motion can be also controlled by the patients' themselves. On the other hand, the handling of deformable motion is more complicated because deformable motion cannot be modeled as a linear process and it is difficult to control by the patients [5]. Breathing is a typical deformable motion that occurs during magnetic resonance imaging (MRI), which can be avoided conventionally by breath-holding. On the other hand, the breath-holding technique is very inconvenient for patients and it cannot be applied to infants or patients with severe diseases [6]. Therefore, a suitable method to handle deformable motion artifacts is needed so

that the deformed region (or non-rigid region) due to breathing can be detected and corrected in the post-processing stages. This paper presents a detection method of deformed regions in radial MRI based on the periodicity of the breathing motion in the projection (Radon transform) and the filtered back-projection (inverse Radon transform) processes.

## 2. Materials and Method

Fig. 1 presents the proposed concept. In radial MRI, the projection reconstruction method can be used to reconstruct an image. The k-space data is converted to a sinogram using a one-dimensional Fourier transform (1D-FT), and then the projection data (sinogram) is transformed into an image by filtered back-projection (FBP). When the projection reconstruction method is used, the final image has an averaged characteristic of all projection views, which can be explained briefly as follows [7]. MR signal corresponding to the 2D line-integral projection at a given projection view,  $\phi$ , is given by

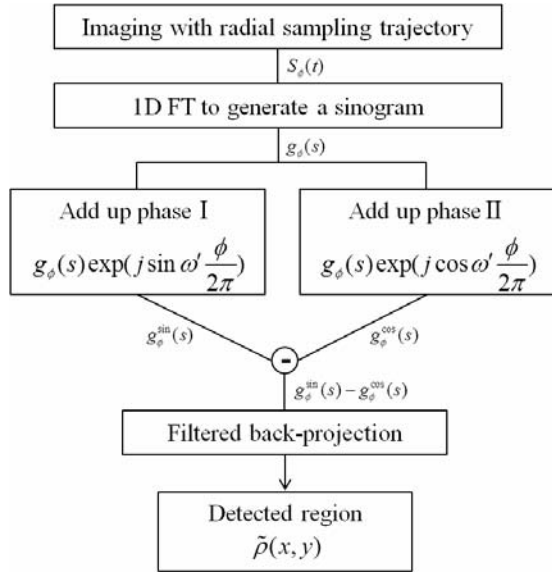


Fig. 1. Concept of the proposed method.

$$S_\phi(t) = \int_s \rho(x, y) \exp(-j\gamma G_\phi s t) ds,$$

$$\text{where } \begin{bmatrix} s \\ u \end{bmatrix} = \begin{bmatrix} \cos \phi & \sin \phi \\ -\sin \phi & \cos \phi \end{bmatrix} \begin{bmatrix} x \\ y \end{bmatrix}, \quad (1)$$

$\rho(x, y)$  is the spin density function of a selected slice, and  $G_\phi$  is a view angle dependent field gradient. Based on Eq. (1), the projection data  $g_\phi(s)$  with a view angle  $\phi$  is calculated as follows:

$$F^{-1}[S_\phi(t)] = g_\phi(s), \quad (2)$$

where  $F^{-1}[\cdot]$  denotes for the inverse 1D-FT. A final reconstructed image is given by

$$\tilde{\rho}(x, y) = \int_0^\pi g_\phi(s) * \zeta(s) d\phi, \quad (3)$$

where  $*$  is a convolution operator and  $\zeta(\cdot)$  is a filter kernel, operating as a high pass filter.

When the radial MRI is performed for a deformable object, each projection data is acquired at different time-points, meaning that the projection data at a specific projection view is acquired from an object with different shape information according to the time of data acquisition. Because the FBP of the sinogram,  $g_\phi(s)$ , is an integration of all projection data, which are acquired while the shape of the target object is constantly changing, the final image contains the averaged information of the patient motion.

In the proposed method, a special characteristic of the average information is used. That is, the signal is cancelled out under a certain condition and is not cancelled under the other conditions. To utilize this characteristic, the sinogram can be modified using the sine and cosine signals

with an angular frequency of  $\omega'$  as follows:

$$g_\phi^{\sin}(s) = g_\phi(s) \exp(j \sin \omega' \frac{\phi}{2\pi})$$

$$g_\phi^{\cos}(s) = g_\phi(s) \exp(j \cos \omega' \frac{\phi}{2\pi}). \quad (4)$$

When the sinogram is modified by Eq. (4), the characteristics of the sinograms are modified as follows; the contribution of the sine or cosine modulation can be summarized as a constant magnitude with a periodically varying phase value. In other words, the change in the magnitude of the sinogram can be expressed as the multiplication by a constant value, but the phase of the sinogram is varied. In addition, the intensity and position of the sinogram corresponding to a rigid region changes moderately with respect to the projection view, so that average or integration of sinograms modulated by sine or cosine signals results in similar values with a phase difference of  $\pi/2$ . This is because the phase variations caused by sine and cosine modulations tend to be periodic and symmetrical, and the difference between the sine and cosine modulations appears as a phase shift. On the other hand, the deformed region causes a discontinuity in the sinogram so that the phase variations appear as a noticeable difference in the sine and cosine modulations, thereby causing a significant difference according to the projection view. As a result, the integration results of the sinograms modulated by the sine and cosine signals are no longer similar to each other.

Based on these modified sinograms, an image ( $\tilde{\rho}(x, y)$ ) can be calculated from the filtered back-projection of the difference sinogram ( $g_\phi^{\sin}(s) - g_\phi^{\cos}(s)$ ) as follows:

$$\tilde{\rho}(x, y) = \int_0^\pi [g_\phi^{\sin}(s) - g_\phi^{\cos}(s)] * \zeta(s) d\phi. \quad (5)$$

Because the FBP results of  $g_\phi^{\sin}(s)$  and  $g_\phi^{\cos}(s)$  are similar to each other in the rigid regions,  $\tilde{\rho}(x, y)$  approaches zero in the rigid regions. On the other hand, these results are not similar in the deformed regions and the reconstructed image of  $\tilde{\rho}(x, y)$  tends to have high intensity on the deformed regions. Consequently, the deformed region can be detected by the additional morphology or threshold operators applied to the reconstructed image,  $\tilde{\rho}(x, y)$ .

### 3. Results and Discussions

A computer simulation was performed using MATLAB (MATLAB 7.10.0.499, The MathWorks Inc., Natick, MA) to verify and analyze the proposed method.

Fig. 2 shows a simulation model consisting of two circles. Although one is the inner circle with a radius  $r$  remaining motionless, the other is the deformable inner

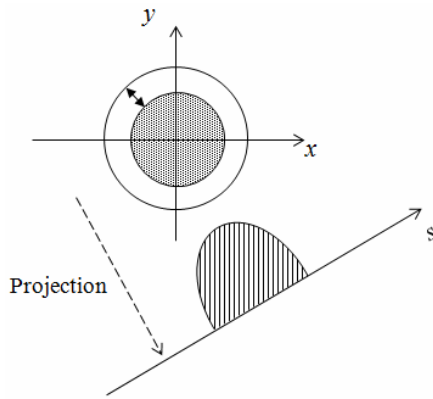


**Fig. 2. Simulation model composed of two circles. The inner circle filled with gray dots is a rigid region and the outer circle is the boundary of the deformable region.**

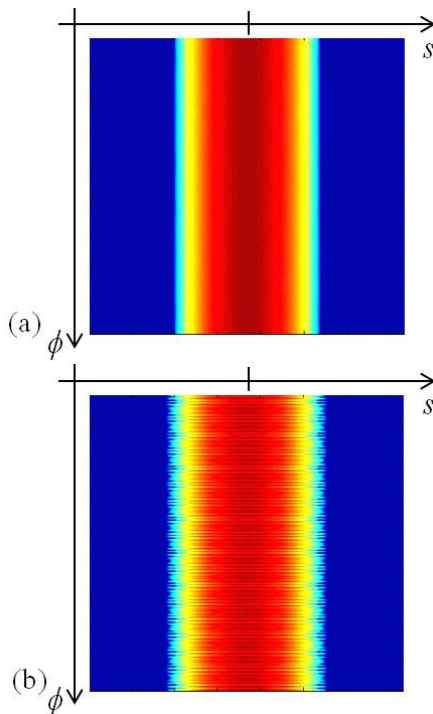


**Fig. 3. (a) Sinogram of rigid circle in Fig. 2, (b) Sinogram containing the deformable region.**

circle whose boundary is deforming periodically with a frequency  $\omega$  to mimic the respiratory motion. The sinogram of the rigid inner circle,  $g_{i,\phi}(s)$  can be represented as  $g_{i,\phi}(s) = 2\sqrt{r^2 - s^2}$ ,  $(-r \leq s \leq r)$ , and the sinogram of moving circle whose boundary is the outer circle,  $g_{m,\phi}(s)$  can be expressed as

$$g_{m,\phi}(s) = 2\sqrt{\left( r + a_1 \left\{ a_2 - \exp\left[ \sin\left( \omega \cdot \frac{\phi}{2\pi} \cdot TR \right) \right] \right\} \right)^2 - s^2}, \quad (6)$$

where  $a_1 \{ a_2 - \exp[\sin(\omega \cdot \frac{\phi}{2\pi} \cdot TR)] \}$  is the movement of a periodic respiratory motion, which was modeled by fitting process of a periodic respiratory pattern acquired from the DC gating of MR experiments [8]. In Eq. (6),  $a_1$  and  $a_2$  are the parameters to determine the deformable range of moving circles.  $TR$  is the repetition time of the MR experiment, and  $\phi/(2\pi) \cdot TR$  denotes that a different motion state is selected at the time of each data acquisition. In this experiment,  $\omega'$  for the angular frequency of the modulation in Eq. (4) was  $0.8\pi$  (rad/s),  $\omega$  was 1 (rad/s) and  $TR$  was 1 (sec) for simple analysis, the radius,  $r$ , was 10 (cm), and  $a_1$  and  $a_2$  were 5 and 2.5, respectively. Therefore, the deformable range of the radius was within 2 (cm). As shown in Fig. 3, when the moving circle is deformed periodically, discontinuities are observed in the sinogram of Fig. 3(b), whereas the sinogram generated from a static circle is constant, as shown in Fig. 3(a). Because the rigid regions are unaffected by both the sine and cosine modulations, the rigid region can be distinguished from the deformed region in the reconstructed image of  $\tilde{\rho}(x, y)$  in terms of the intensity.

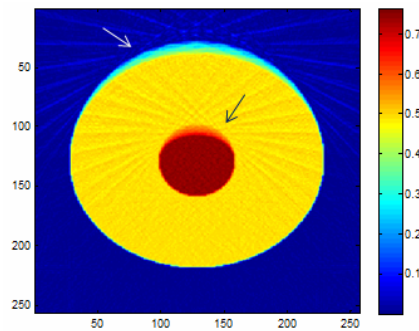


**Fig. 4. Simulation phantom, which has the similar boundary shape and respiratory pattern to the abdomen. The two arrows indicate the deformable region.**

Based on these characteristics, the proposed method was applied to a different body model using the above mentioned respiratory model. The parameters of the simulation are as follows:  $\omega'$  for angular frequency of the modulation was  $0.8\pi$  (rad/s),  $\omega$  was  $0.4\pi$  (rad/s) to reflect the respiratory period of 5 (sec),  $TR$  was 2 (sec), and  $a_1$  and  $a_2$  were 5 and 2.5, respectively. Long ( $r_1$ ) and short ( $r_2$ ) axes of an ellipse were 30 (cm) and 20 (cm), respectively. The motion of the inner circle with a radius of 5.5 (cm) was the same as the outer ellipse. Fig. 4 shows the image used in the simulation. As revealed by the difference in magnitude image in Fig. 5(a) and the difference in phase image in Fig. 5(b), the rigid region has intensity values close to zero and the deformed regions have higher intensities. Therefore, using the difference images in Figs. 5(a) and (b), the deformed region extracted by the threshold value is 35 % of the maximum intensity of the respective difference images. Fig. 6 shows the results of the proposed method applied to a different simulation

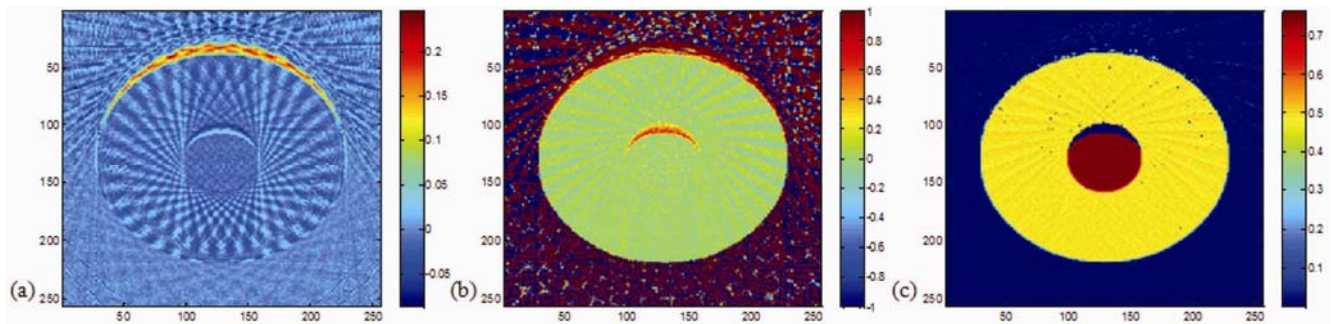


**Fig. 5. (a) Result image, which is difference of magnitude images generated from sinogram modulated by sine and cosine, (b) Result image which is difference of phase images generated from sinogram modulated by sine and cosine, (c) Extraction of deformed region using the result of Fig. 4 (a) and (b).**

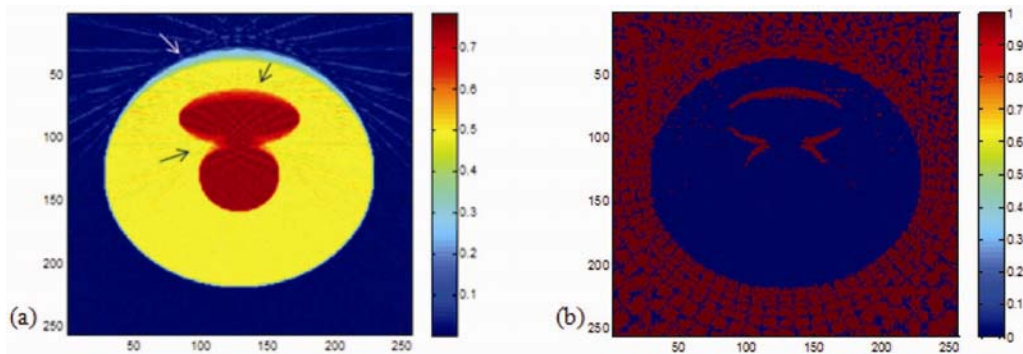


**Fig. 6. (a) Another phantom in the case of two adjacent deformable objects. The arrows present the deformable region, (b) Mask made using the proposed method.**

model composed of two adjacent objects with deformed regions with the same motion. The model in Fig. 6 was added an additional ellipse, whose  $r_1$  was 7 (cm) and  $r_2$  was 3 (cm), to the model used in Fig. 4. From the extraction result shown in Fig. 5(c), PSNR was measured and compared with a gold standard image based on Fig. 4 without motion. The PSNR was 76 dB and the proposed method was expected to be used effectively for the extraction of actual respiratory motion in the body.

The proposed method needs to be validated for *in-vivo* imaging to be optimized for actual motion artifacts, motion estimation and correction. Therefore, further work will involve experiments with real MR data as well as more accurate analysis of the proposed method.

## 4. Conclusion

A detection method of deformable motions in radial MRI was proposed. The proposed method did not require a priori information regarding the motion or complicated processing algorithms. The method only added the periodic phase information according to the projection views in the sinogram domain to allow the rigid and deformed regions to be distinguished as an intensity difference. The performance of the proposed method was verified by simulations of a range of models of the deformable motion.

## References

- [1] M. L. Wood and R. M. Henkelman, "MR image artifacts from periodic motion," *Med Phys*, 1985. [Article \(CrossRef Link\)](#)
- [2] D. R. Bailes, D. J. Gilderdale, G. M. Bydder, A. G. Gollins, and N. F. Firmin, "Respiratory ordered phase encoding (ROPE): a method for reducing respiratory motion artifacts in MR imaging," *J Comput Assist Tomogr*, 1985. [Article \(CrossRef Link\)](#)
- [3] E. M. Haacke and J. L. Patrick, "Reducing motion artifacts in two-dimensional fourier transform imaging," *Magn Reson Imaging*, 1986. [Article \(CrossRef Link\)](#)
- [4] Yasser M. Kadah, Ayman A. Abaza, Ahmed S. Fahmy, Abou-Bakr M. Youssef, Keith Heberlein, and Xiaoping P. Hu, "Floating navigator echo (FNAV) for in-plane 2D translational motion estimation," *Magn Reson Med*, Feb. 2004. [Article \(CrossRef Link\)](#)
- [5] Martin Buehrer, Jelena Curcic, Peter Boesiger, and Sebastian Kozerke, "Prospective self-gating for simultaneous compensation of cardiac and respiratory motion," *Magn Reson Med*, Sep. 2008. [Article \(CrossRef Link\)](#)
- [6] Anja C. S. Brau and Jean H. Brittain, "Generalized self-navigated motion detection technique:

Preliminary investigation in abdominal imaging,” *Magn Reson Med*, Feb. 2006. [Article \(CrossRef Link\)](#)

- [7] Y. Han, JY. Hwang, JY. Jung, S. Yun, and HW. Park, “Improvement of the Diffusion-Weighted Images Acquired With Radial Trajectories Using Projection Data Regeneration,” *J Magn Reson Imaging*, 2007. [Article \(CrossRef Link\)](#)
- [8] Stefan Weick, Felix A. Breuer, Volker Michael, Hintze Christian, Biederer Jurgen, and Jakob Peter M., “DC-Gated High Resolution Three-Dimensional Lung Imaging During Free-Breathing,” *J Magn Reson Imaging*, 2013. [Article \(CrossRef Link\)](#)



**Hyunseok Seo** received his B.S. degree from Korea University, Korea in 2011 and the M.S. degree electrical engineering from KAIST, Korea in 2012. He is pursuing a PhD degree in the Department of Electrical Engineering, KAIST. His research interests include signal processing,

image processing, and medical imaging regarding image reconstruction and MRI pulse sequence.



**HyunWook Park** received his B.S. degree in electrical engineering from Seoul National University, Seoul, Korea, in 1981, and M.S. and Ph.D. degrees in electrical engineering from the Korea Advanced Institute of Science and Technology (KAIST), Seoul, in 1983 and 1988, respectively.

Since 1993, he has been a Professor with the department of electrical engineering, KAIST. He was the department head of electrical engineering with KAIST from December 2005 to January 2011. Since 2003, he has been an Adjunct Professor with the department of bio and brain engineering, KAIST. He was a research associate with the university of Washington, Seattle, from 1989 to 1992 and was a Senior executive Researcher with Samsung Electronics Co., Ltd., Seoul, from 1992 to 1993. His current research interests include image computing systems, image compression, medical imaging, and multimedia systems. Dr. Park has served as an associate editor for the International Journal of Imaging Systems and Technology.